Characterisation of cooled infrared fibres for the Gemini IRMOS

Roger Haynes[+], Ivan K. Baldry, Keith Taylor, David Lee

Anglo-Australian Observatory, 167 Vimiera Road, Epping NSW 2122, Australia

ABSTRACT

Recently integral field spectroscopy has become a band-wagon among the optical astronomical community and most of the 8m class telescopes plan to offer this as part of their instrumentation package. The possibility of expanding integral field spectroscopy into the near infrared (1-2.5μm) opens exciting new possibilities for the study of a variety of astronomical objects.

In this paper, we discuss some of the design requirements for the proposed Gemini Infra-Red Multi-Object Spectrograph (GIRMOS) and sky subtraction techniques suitable for infrared fibre spectroscopy. We address the performance of optical fibres suitable for use from 1-2.5μm and the effects of cooling these fibres to liquid nitrogen temperatures (~77°K) including: focal ratio degradation (FRD), fibre transmission and thermal emissivity, mechanical properties and durability. Also discussed are issues related to sky subtraction for IR fibre spectroscopy such as: dedicated sky fibres, dedicated sky d-IFUs, and various beam switching methods. This work is all part of a development study for multiple deployable integral field units (d-IFUs) for GIRMOS.

Keywords: GIRMOS, cryogenic infrared fibres, infrared spectroscopy, integral field units, multi-object spectrograph

1. INTRODUCTION

Over the past decade most of the 4m class telescopes have developed multi-object spectrographs to observe at optical wavelengths (0.3-0.9μm)[7,20]. These have been based on either multiple fibres or multiple slits and have dramatically increased the efficiency of observing by up to factors of 100 or greater. This has facilitated large surveys that have provided valuable statistical samples of various astronomical objects. The extension of these multi-object techniques into the infrared has been impeded by the lack of suitably large detectors. However, with the recent development of 1K x 1K HgCdTe and InSb arrays, and with the prospects of 2K x 2K and large arrays[10], it is now possible to extend these techniques into the infrared. A number of instruments are currently being built to this very purpose based around cooled multi-slits[6]. However, multi-slit spectroscopy is best suited to point sources and some interesting possibilities arise if one is able to efficiently observe extended objects.

To this end the GIRMOS[26,27] development study is investigating technologies that will enable multi-object integral field spectroscopy in the near-infrared (1-2.5μm) based on either image slicers[2,17,25] or fibre IFUs[8,9,12,13,21]. A collaboration between the Anglo-Australian Observatory, the UK Astronomical Technology centre (UKATC) Edinburgh and the University of Durham has been formed, each addressing specific technical challenges associated with moving to the infrared. There is a paper[27] presented in these proceedings describing the work being carried out by UKATC and Durham.

Because of the thermal background considerations, it is necessary to cool most of the instrument if you operate at wavelengths beyond 1.7μm. It is also necessary to operate at reasonably high spectral resolution in order to work between the OH airglow lines, with suitable R typically in the range from 2000-6000. One also requires extremely good sky subtraction to eliminate the stronger OH lines and effectively handle the intra-line and thermal continuum.

The aim of this paper is to present the work being carried out at the Anglo-Australian Observatory into infrared fibre deployable integral field units (d-IFUs) for Gemini, including the characterisation of infrared fibres and sky subtraction issues.

[+] Correspondence: Email rh@aaoepp.aao.gov.au: WWW http://www.aao.gov.au; telephone: +61 2 9372 4815;
Fax: +61 2 9372 4880

2. GIRMOS FIBRE D-IFU OUTLINE

The science aims of the GIRMOS d-IFUs include the study of: the initial mass function in obscured star formation regions; young stellar object jets, protostars, etc; embedded star clusters or starburst clumps; star formation regions in high redshift galaxies; and gravitational lensing. To facilitate such studies the instrument requirements outlined below have been proposed. The study does not involve the complete design of an instrument, however it is important that every effort should be made to ensure that the components under investigation do not significantly limit the performance of such an instrument.

2.1 Wavelength range

The wavelength range of the d-IFUs is from 1-2.5μm and suited to both InSb and HgCdTe detectors. However, this has strong implications for the type of infrared fibres that can be considered. It also pushes the specification into the thermal regime where cooling of most of the spectrograph components and careful baffling of the optical train is necessary to keep the thermal background to levels well below that of the sky and telescope.

2.2 Sensitivity and spectral resolution

The instrument sensitivity is to be limited by sky continuum (i.e.. excluding the strongest OH lines) over greater than 75% of the J and H bands, and limited by telescope and atmospheric thermal background in the K band. This implies a spectral resolution (R) ~ 6000 and as part of the GIRMOS study, the IOA are addressing the exciting prospect of cold volume phase gratings. Also to ensure good S/N spectra, carefully consideration should be taken of sky subtraction techniques. The throughput stability of the d-IFUs should be better than 1% to enable accurate sky subtraction for all bands. Both the implications of spectral resolution and sky subtraction techniques are discussed later on.

2.3 Scattered light

The amount of scattered light falling on the detector will have a large impact on the sensitivity of the instrument because of the strong OH lines present in the J and H bands. This leads to the requirement that less than 5% of this strong OH lines flux should illuminate the detector as uniformly scattered background.

2.4 Spatial sampling, field of view and number of d-IFUs

The number of d-IFUs is to be somewhere between 10 - 20. This number will of course depend on: the detector real-estate (i.e. the number of pixels available to sample to d-IFU output slits), currently 4K x 4K detector pixels are envisaged; critical sampling of the individual fibres and spectral overlap considerations (this is not so critical if fibres that are spatially adjacent at the input, are also spatially adjacent on the detector); the size of sampling element and field of view (FOV) of the d-IFUs.

There are two spatial resolutions being considered for the d-IFUs. The first is low resolution with a 0.15 arcsec sampling and a 3 arcsec FOV. The d-IFUs will be well suited to the uncorrected image quality available at Gemini North and will be deployable over at least a 5.5 arcmin field, but cover the full potential 10 arcmin if feasible. The second is higher resolution with a 0.03 arcsec sampling resolution and a 2 arcsec field of view. The higher resolution will be well suited to the image quality provided by the multi-conjugate adaptive optics (MCAO) system available at Gemini South supplying a 2 arcmin corrected field.

2.5 d-IFU robot positioner

With the relatively small field, small numbers of d-IFUs and the cryogenic environment, it was felt that the “fishermen around a pond” approach for the positioner would be most suitable (Figure 1). Each d-IFU probe is able to both piston and rotate, enabling access to the sector between adjacent probes. The system should be capable of accessing more than 50% of randomly distributed targets, given a target number similar to the total number of d-IFUs. For a single pair of targets, the minimum achievable separation should be less than 10 arcsec in low-resolution mode and less than 3 arcsec in high-resolution mode.

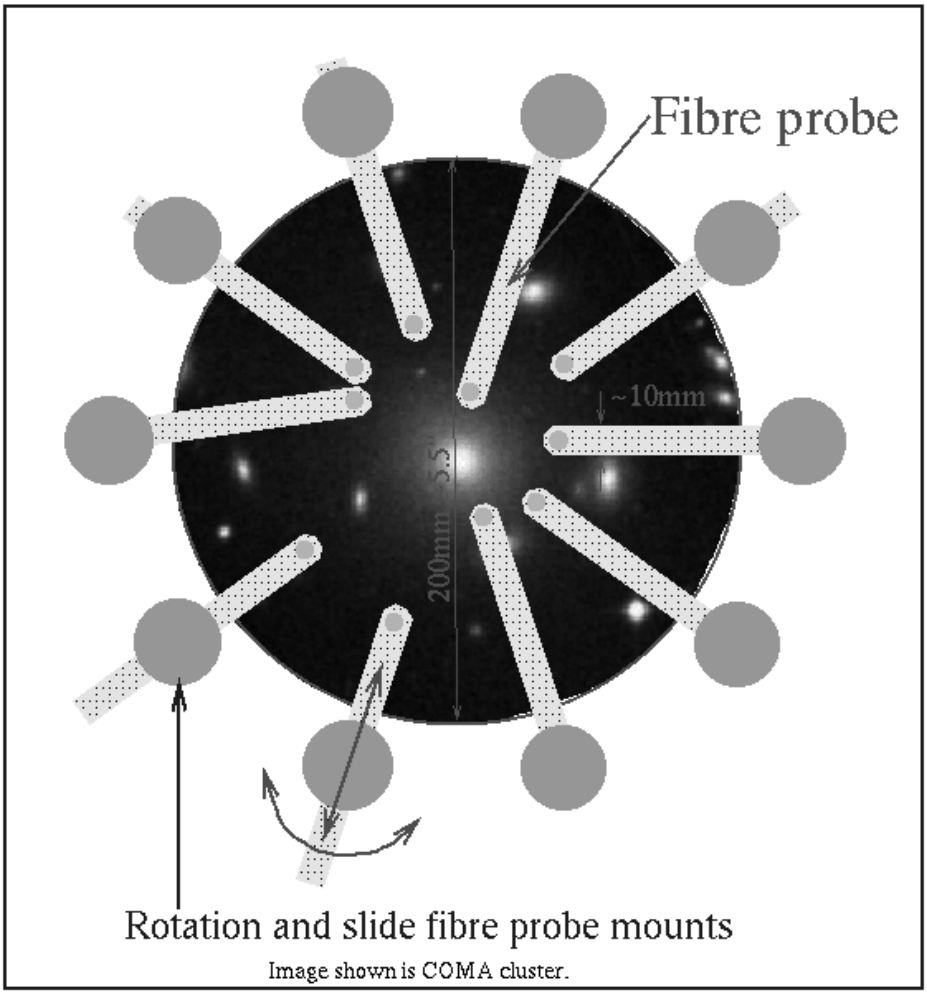

Figure 1: Schematic of the GIRMOS fibre d-IFU positioner superimposed over the COMA cluster

The absolute placement accuracy of each d-IFU, for both high and low-resolution modes, should be better than 1/5 of the d-IFU field of view. This relatively loose specification is possible because the image on the d-IFU can be reconstructed in software and provide the valuable acquisition information. However, once deployed the d-IFU input should have less than $1/10^{th}$ pixel flexure over a tracking period of 2 hours.

Re-configuration times between one object field and the next should be less than 10 minutes.

A more detailed mechanical development of this concept is currently under way addressing these constraints in the technically challenging cryogenic environment, looking into materials, drive mechanism, probe design and positioner geometries. At this stage in the design it is not desirable to preclude installing this unit inside the main spectrograph and for it to operate at ~77°K. However, as far as thermal background considerations are concerned, it is not really necessary to cool the fibre probes below about 170°K when operating out to wavelengths of 2.5μm. A further complication involves compensating for the curved focal plane (r~1.9m) of the telescope, which will may be resolved using field flattening optics.

2.6 d-IFU probe

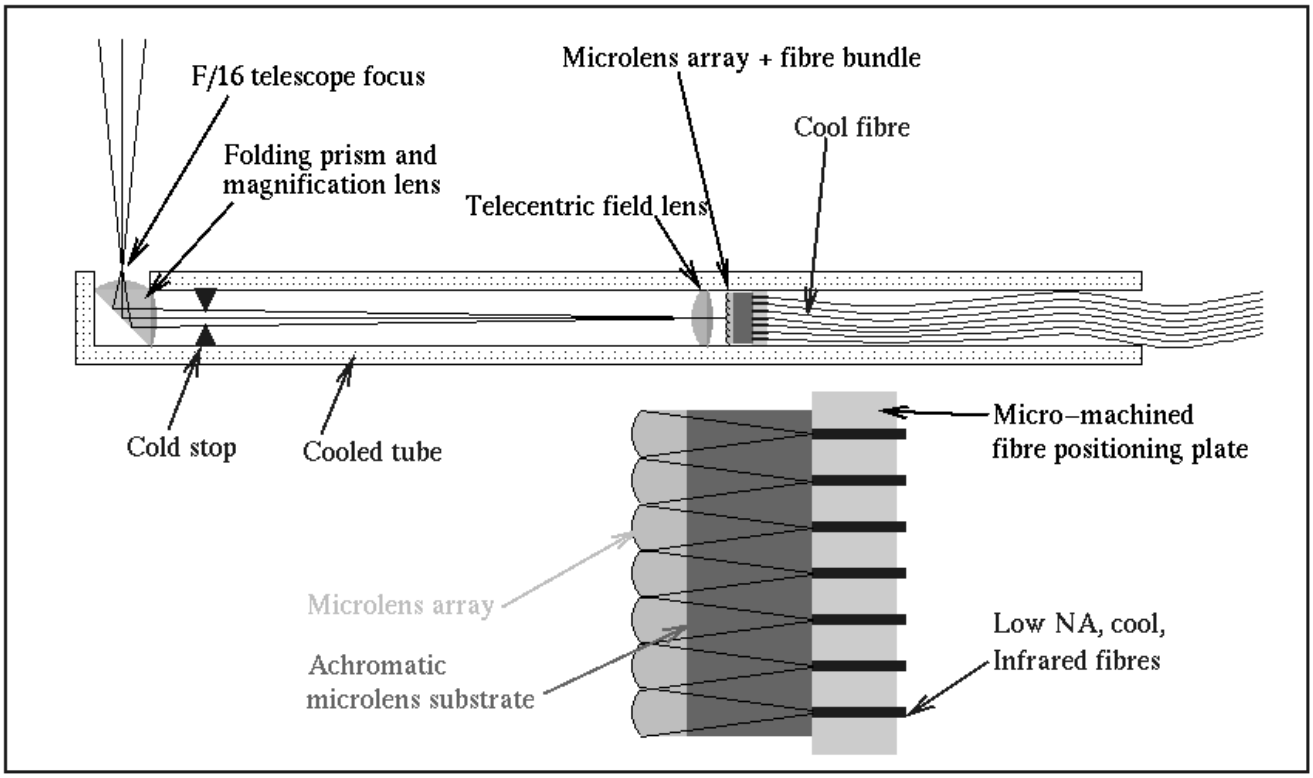

Figure 2: A schematic of a d-IFU probe.

The d-IFU probe consists of a self-contained "pencil" style unit that addresses the object field just below the f/16 telescope focal plane. The image is picked off from the focal plane by a 45° prism. In an effort to reduce the number of surfaces this is combined to form the magnification lens. A cold pupil stop is included to mask contribution from the telescope structure and sky around the telescope pupil (for Gemini this is the secondary mirror). A telecentric field lens is used to correct the beam, before feeding onto the microlens array. This magnification fore-optics allows much greater flexibility in microlens choice and can have the benefit of reducing geometric focal ratio degradation (FRD) introduced by the microlenses. However, given a suitable microlens array it would also be possible to feed the microlenses using just a 45% prism and no magnification optics.

Most microlens arrays do not produce a focus on their output face so an achromatic substrate is used to correct chromatic aberration and alleviate the need for a further two air-glass surfaces. The light is fed into the fibre at ~f/7.5, which would be equivalent to about f/5 in air. However, this f/ratio depends critical on the FRD performance of the fibres, the minium useable fibre core size, the sampling scale and the image to fibre core ratio. Many of these factors are still under investigation. As part of the study a number of microlenses from various manufactures (Limo, MEMS & AOA) are being tested to access their fill factor, image quality and scattered light characteristics. These can critically effect the coupling losses, both into and out of the fibre, through the rest of the spectrograph.

To provide efficient coupling and reduce the over sizing requirements of the fibre core, the fibres are accurately positioned on a pitch matching that of the microlens array. A number of techniques and materials for the positioning the fibres are being investigated. The most promising so far is micro-drilled machineable ceramic hole arrays.

As the system wavelength range is 1-2.5μm, it is not possible to use silica based fibres, except in very short lengths (>>1m) so, specialised infrared fibres must be used. This is discussed later in this paper. The fibres feed from the positioning plate and re-format into pseudo slit at the focal plane of the spectrograph. The input requirements of the spectrograph have not yet been finalised so it may be possible to feed it with the raw fibre output, which is expected to be f/4 or slower. However, if the

spectrograph requires a slower input beam it may be necessary couple the fibre outputs using linear microlens arrays, converting to a suitable f/ratio to give high throughput. The fibre-to-fibre spacing at the output will be determined as a function of the critical sampling of spectrographs image quality, scattered light consideration and the desire to maximise the number of fibres and hence number of the d-IFUs. A possible trade-off could be to reduce spectral coverage for multiple fibre slits spaced along the dispersion direction (ie: two slit would double the number of d-IFUs, but half the spectral coverage accessible without overlap). Some of these could be masked off, to give high spectral range, but reduce numbers of d-IFUs available to sample the field. Another technique for improving the spectral coverage/resolution is dithering of the detector.

3. FIBRE CHARACTERISTICS

When considering fibres for GIRMOS there are a number of both optical and mechanical attributes to be tested.

1. Transmission of the fibre over the operating wavelength range of 1-2.5μm. This also gives an indication of the thermal emissivity of the fibre ($\varepsilon \sim 1/T$), where ε is the emissivity and T is the transmission.
2. Focal Ratio Degradation (FRD) characteristics when fed with the raw f/16 Gemini beam and when coupled with microlenses which is expected to be about f/5. FRD, both fibre and geometric (e.g. a square lens provides a faster f/ratio across the diagonals than across the flats), translates into loss in AΩ product and thereby a potential loss in system performance.
3. Mechanical flexibility and minimum useable bend radius. This can have a significant impact on FRD and at the extreme limits the transmission of the fibres.
4. Mechanical robustness and durability, which could severely impact on the probe design. The current design assumes a simple system in which the fibres flex as the probes move. However, UKATC have a proposed a system[26,27] that involves a constant path length pick off system of mirrors that feed fixed IFUs, which could be employed if necessary.

In order to allow maximum flexibility in the spectrograph design, these tests are being carried out at the minimum expected operating temperature of the dewar (~77°K) and at room temperature. The later allowing comparison with results from previously tested fibres.

3.1 Fibre Transmission

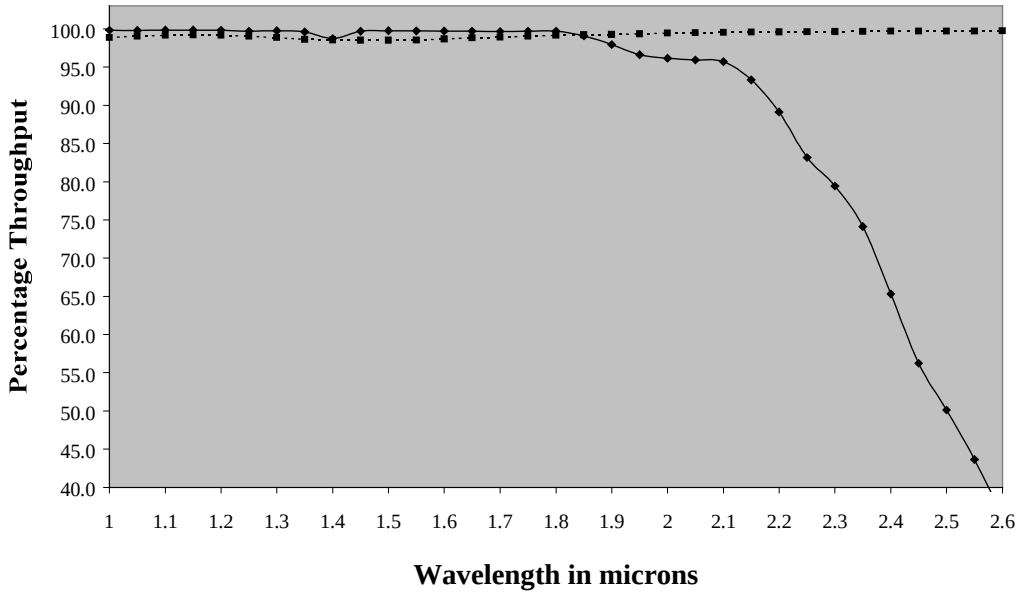

Figure 3: Transmission (from the manufactures data) of the 1m length of fibre, not including Fresnel's reflection end losses. The diamonds are a typical low OH silica fibre (Si) from Polymicro Technologies Limited and the squares are a typical zirconium fluoride (ZrF_4) fibre from Le Verre Fluore.

In figure 3 it can be clear seen that a low OH silica (Si) fibre has excellent transmission from 1-1.8μm (T > 99%), but it starts to drop off rapidly beyond about 2.1μm and is ~ 50% at 2.5μm. The ZrF_4 fibre has slightly worse transmission from 1-1.8μm (T~99%), but does not show the drop off over the rest of the wavelength range (T > 99% at 2.5μm). This implies, that unless very short lengths of silica fibre are used (<0.3m, T~80% at 2.5μm), it is necessary to use zirconium fluoride fibres to efficiently access the full K band. It is expected that the GIRMOS fibres will be at least 0.5m long, unless the UKATC style mirror pick off units are employed with fixed fibre IFUs. In the later case, the fibre length may be short enough to consider silica fibres. If these fibres were at room temperature, the increased thermal emission resulting from the drop in transmission could degrade system performance, however cooling the fibres would make this negligible. As part of the GIRMOS d-IFU study, the transmission of both ZrF_4 and Si fibres will be determined at room and liquid nitrogen temperatures.

3.2 Focal ratio degradation characteristics of the fibres

The FRD characteristics of four different fibres where tested with both a f/5.5 input beam, corresponding to the fibres being fed by microlens and a f/16 input beam, corresponding to the "raw" telescope beam. These were:

1. 1m length of IR Guide-1 ZrF_4 fibre (**IRG80**) with a 80μm core, 88μm cladding and 96μm acrylate buffer, supplied by Le Verre Fluore (France).
2. 1m length of SG 100/150/163 ZrF_4 fibre (**SG100**) with a 100μm core, 150μm cladding and 163μm polyimide buffer, supplied by Infrared Fiber Systems Inc (USA).
3. 1m length of FIP040/056/066 low OH silica fibre (**FIP40**) with a 40μm core, 56μm cladding and 66μm polyimide buffer, supplied by Polymicro Technologies Ltd (USA).
4. 2m Length of FVP100120140 high OH silica fibre (**FVP100**) with a 100μm core, 120μm cladding and 140μm polyimide buffer, supplied by Polymicro Technologies Ltd (USA).

The IRG80 and SG100 where the only suitable "off the shelf" fibres available at the time of ordering. As only short length of fibre where required, custom fibres would have been prohibitively expensive at this stage of the study. The cladding size of the IRG80 is not ideally suited to infrared transmission. As a rule of thumb, the cladding should be rough 10x the maximum operating wavelength, otherwise the evanescent waves are not sufficiently contained with the cladding and losses can occur.

The FIP40 fibre was chosen as a small core "multi-mode" fibre. This is because, if you assume f/5 microlens coupling on GIRMOS, the image size on the fibre input face corresponds to a ~30μm & 6μm for 0.15" & 0.03" sampling respectively (not including diffraction or any image degradation). It should be noted that a 6μm core fibre is too small for multi-mode operation. The FVP100 provides a comparison within a typical fibre used in many optical fibre systems.

All the fibres, except the FVP100, were dry polished using 3M imperial lapping film. The dry polishing is necessary for ZrF_4 fibres as they are slightly hydroscopic and the performance can degrade in the presence of water. The FVP100 fibre was prepared on a Kent "Lapmaster" polishing machine, using a cast iron lapping plate with 9μm, followed by 3μm aluminium oxide lapping slurry, then polished on a polyurethane polishing plate using a 0.03μm colloidal silica polishing suspension.

3.2.1 "Warm" FRD tests at optical wavelengths

A series of test were carried out at room temperature on the four test fibres, using a tungsten halogen light source, that fed through a source fibre, its output was then re-imaged onto the test fibre face at the appropriate f/ratios. A fibre mode scrambler was used to ensure uniform illumination and eliminated any structural artefacts from the light source. The output from the test fibre was then re-imaged onto a photodiode and the f/ratio illuminating the diode was varied by a series of different size apertures, that "stopped down" the fibre output beam.

In Figure 4, It can be seen that the "warm" optical FRD characteristics of the ZrF_4 fibres are at least as good if not better than the silica fibres. SG100 has ~88% of the output energy enclosed within a f/5.5 beam and IRG80 ~ 77%. The results for the silica fibres are slightly worse, FIP40 has ~ 70% and FVP100 ~ 68%. These FIP40 and FVP100 results are reasonably typical for silica fibres. The FVP100 fibre has a slightly different profile than the other fibres, but is consistent with previous measurements and may be the result of the fibre core not being polished perpendicular to the fibre face. Further tests using a 1m dry polished length of this fibre are currently being processed, along with the effects of fibre bend radius.

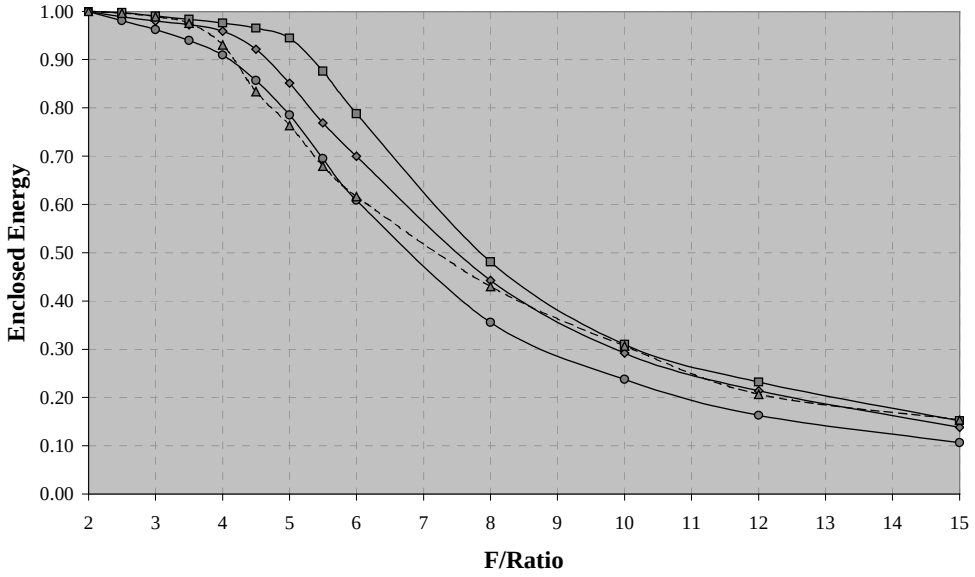

Figure 4: Optical wavelength, focal ratio degradation curves for "warm" fibres fed with a f/5.5 input beam. The squares are SG100 fibre, the diamonds are IRG80, the circles are FIP40 and the triangles are FVP100 fibre. The curves have been normalised to 1 at f/2, which was the limit of the detector system. This is slightly faster than dictated by the numerical aperture of the fibres, also where most of the FRD curves are reasonably flat.

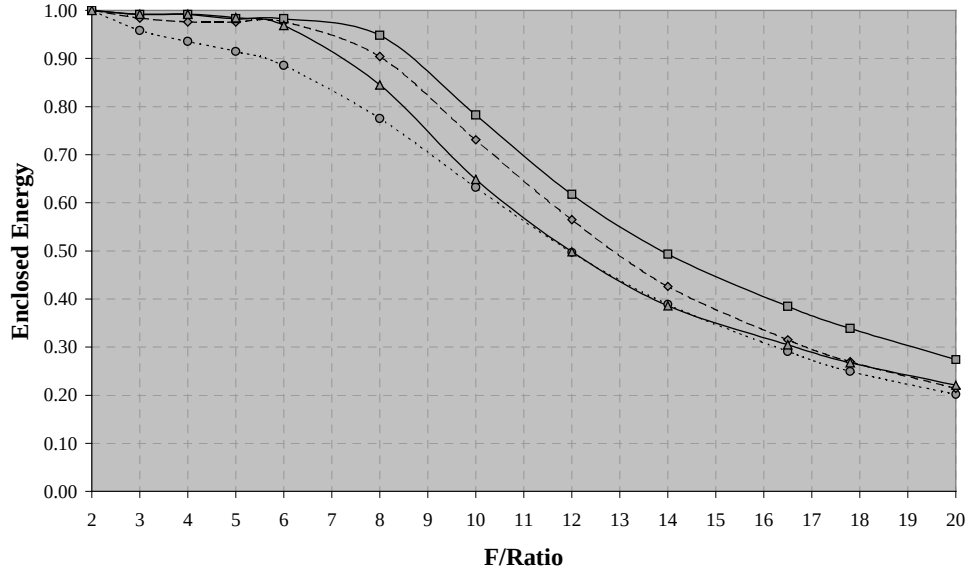

Figure 5: Optical wavelength, focal ratio degradation curves for "warm" fibres fed with a f/16 input beam. The squares are SG100 fibre, the diamonds are IRG80, the circles are FIP40 and the triangles are FVP100 fibre. The curves have been normalised to 1 at f/2.

In Figure 5, It can be seen that again the ZrF_4 fibres are at least as good if not better than the silica fibres. However, the percentage enclosed energy is much less at the f/16 input, than it was at the corresponding f/5.5 input. The SG100 is best again at ~ 40%, the IRG80 is next at ~ 33%, the silica fibres are again worse, with FVP100 ~ 32% and FIP40 ~ 31%.

Brief tests were carried out to investigate how FRD changed with wavelength (within the optical regime) by placing Schott glass filters in the beam. There did appear to be a slight worsening of FRD with increased wavelength. However, this result is tentative at this stage. Tests of the FRD characteristics from 1-2.5μm are under way.

3.2.2 Fibre FRD when cooled.

There is an on going investigation of the FRD performance when cooled to ~ 77°K. Tests have been carried out which show a degradation of the fibre output cone as they are cooled. This is yet to be quantified. It was also noted that the fibres FRD seems to return to roughly the original levels when the fibre warm up. It is not clear whether this worsening is an inherent property of the fibres themselves or whether it is a result of local stressing induced by the fibre termination. It is proposed to clarify this by testing some unterminated fibres. The optimal termination strategy, i.e. that which induces the least stress into the fibres, is an important part of the development study.

3.3 Mechanical robustness and durability

It is known that the mechanical robustness of ZrF_4 fibres is not as good as silica fibres[23], however silica fibres are remarkable robust and durable having been used in numerous astronomical instruments. ZrF_4 fibres have been used in astronomy[3,5,9,14] to a limited extent. However, GIRMOS d-IFUs will work in a demanding environment. They may undergo repeated bending, at cryogenic temperatures. One of the first questions to be addressed was: do silica and ZrF_4 fibres mechanically survive at these temperatures ? The simple answer is, yes. A test was devised in which lengths of IRG80, SG100, FIP40 and FVP100 fibre were tied in a loop and dunked into liquid nitrogen. By alternately pulling and pushing on the fibre ends the cold fibre loop was repeatedly opened and closed. This was achieved without the fibres breaking. Typical loop diameters were between 100mm & 30mm, with loops of down to 10mm possible with breakages. There was slight discolouration of the buffer material after dunking, but no other adverse effects where noted. This was a rather severe test, but it demonstrated that the both the silica and ZrF_4 fibres are mechanically robust and reasonable durable at 77°K. This is consistent with communications received from Le Verre Fluore. The plan is to carry out further durability testing before a prototype d-IFU probe is designed.

4. SKY SUBTRACTION

4.1 Consideration of spectral resolving power

The impact of the infrared sky background on spectroscopic observations (in the range 1.0-2.25μm) is strongly dependent on the resolving power.

In the J and H bands, the sky background is dominated by the night-sky OH emission lines, and at wavelengths longer than about 2.25μm, it is dominated by thermal emission from the sky and telescope. Spectroscopic observations of OH airglow emission have been made by, for example: Maihara et al.[16] in the 1.1-1.8μm range with a resolving power R of 17000; Oliva & Origlia[19] in the 1-2.5μm range with R of about 4000, and; Ramsay et al.[22] in the 1-2.5μm range with R of below 1000. Jones et al.[11] and Offer & Bland-Hawthorn[18] used these various sources to produce a model night-sky spectrum with delta functions for the emission lines (which they could then convolve with filter profiles to test OH-suppression methods).

To quantify the effect of resolving power on spectroscopic observations, in regard to observing between the OH lines, we simulated spectra by broadening the model night-sky spectrum with Gaussian profiles. The spectra were calculated for sampling of three pixels per FWHM of the Gaussian profiles. For a range of resolving powers in the J and H bands, the fraction of spectrum that is effectively clear of OH lines was determined by setting an upper limit on the intensity attributable to OH emission for each pixel. Figures 6 and 7 show the results of these calculations[*]. The resolving powers refer to the middle of the bands, 1.25 and 1.65μm, respectively. The resolution (FWHM of the Gaussian) was assumed constant across each band.

[*] The model sky spectrum included 63 OH lines between 1.15 and 1.35μm and 82 lines between 1.5 and 1.8μm. There are additional OH lines of lower intensity in between these stronger lines, and therefore, the calculated OH-clear fractions are only upper limits. There will also be some effect from scattering which will spread a small fraction of the OH emission across an observed spectrum, this was not considered in the calculations.

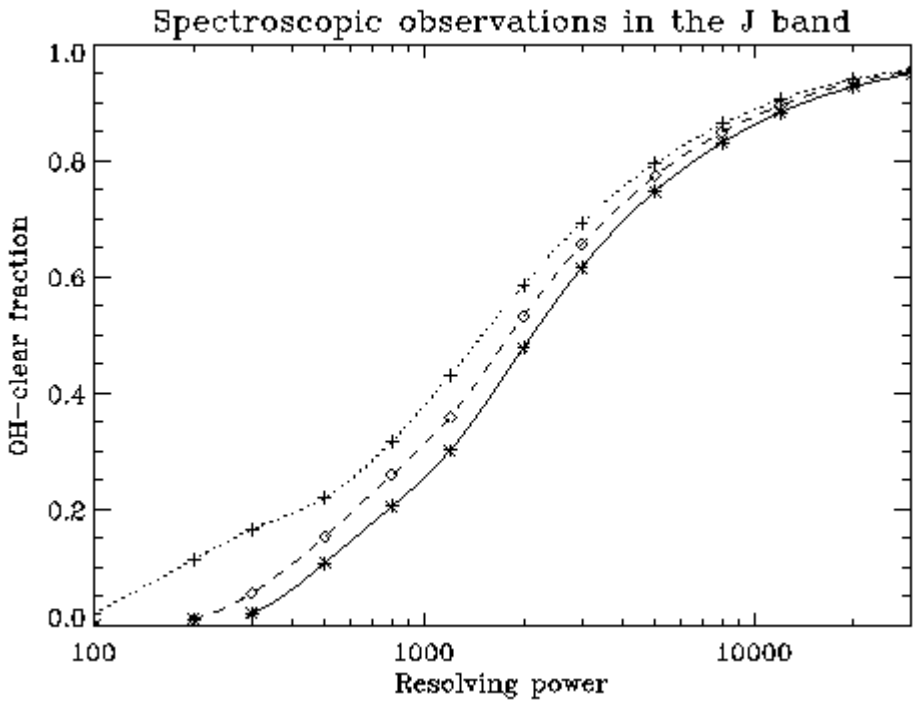

Figure 6: Fraction of a 1.15-1.35μm spectrum that is effectively clear of OH emission. The solid line represents the fraction of the spectrum where less than 60 photons s^{-1} m^{-2} $arcsec^{-2}$ μm^{-1} is attributed to OH emission, while the dashed line and the dotted line represent the fractions where less than 300 and 1000 photons, respectively, are attributed to OH. The calculation was made using a model-sky spectrum and Gaussian profiles, see text for details. Scattered light was not considered. For comparison, Maihara et al.[16] measured the continuum intensity on a dark night to be 590±140 photons s^{-1} m^{-2} $arcsec^{-2}$ μm^{-1}.

Clearly, increasing the resolving power increases the OH-clear fraction up until the OH emission lines are resolved (at R ~ 100 000). To obtain an OH-clear fraction of 0.75 requires a resolving power of about 5000 and 6000 in the J and H bands, respectively. However, to increase the fraction to 0.9 would require the resolving power to be more than doubled. In the lower wavelength half of the K-band (2.0-2.2μm), we would expect similar results (eg., see spectrum in the paper by Oliva & Origlia[19]) - in the other half (2.2-2.4μm), the OH-clear fraction is not important because sky continuum emission dominates.

The ideal resolving power for a particular instrument depends on how much weight is given to the importance of wavelength coverage, the resolving power itself and the OH-clear fraction. For example, if equal weight is given to wavelength coverage (assuming proportional to 1/R) and the OH-clear fraction, then resolving powers of about 1000 and 1500 are suitable for the J and H bands, respectively. However, if some weight is given to the resolving power itself and/or higher weight is given to the OH-clear fraction, then resolving powers of around 2500-5000 and 3000-6000 are suitable. Higher resolving powers are only suitable if the scientific case absolutely requires high resolution, because of the decreased wavelength coverage without any significant gains in the OH-clear fraction.

Sky-subtraction methods

Sky-subtraction with fibres has been discussed by Wyse & Gilmore[28], Cuby & Mignoli[4], Lissandrini et al.[15], Watson et al.[24] and Allington-Smith & Content[1]. Possible sky-subtraction methods for GIRMOS include:

1. dedicating 10% to 20% of the IFUs to the sky (eg. ~4 from 20);
2. having a selection of deployable individual fibres for sky subtraction (10% to 20% of total fibres dedicated to sky);
3. & 3M. switching between all the IFUs on the objects and all on the sky;

4. ‘cross beam switching’ - half the IFUs on objects and half on the sky, such that each object IFU has an associated sky IFU with the same vector displacement between the sky and object for each pair - then, beam switch so that the sky IFUs become the object IFUs and vice-a-versa.

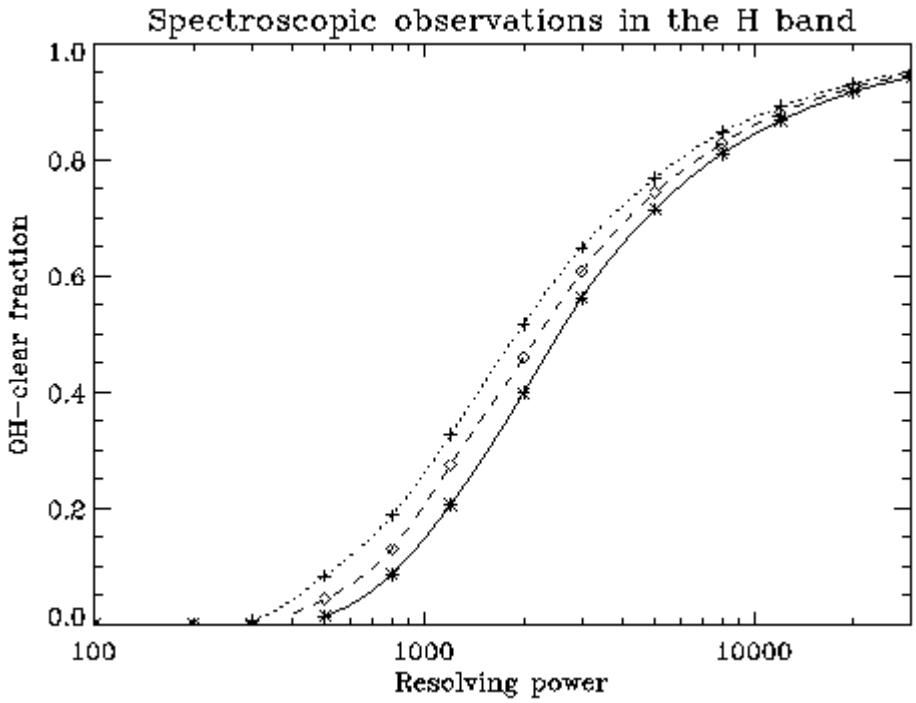

Figure 7: Fraction of a 1.5-1.8μm spectrum that is effectively clear of OH emission. See Figure 6 and text for details.

The first two methods are mean-sky methods. For these methods, the observed spectra from all or most of the sky fibres are combined to produce a single sky spectrum which is subtracted from each object spectrum using appropriate reduction techniques. Accurate wavelength calibration and measurement of fibre transmittance are important.

Methods 3 and 4 are beam-switching methods, each fibre is used to observe object and spectra in alternate exposures (typically, of equal length). Each sky spectrum is subtracted from the object spectrum taken with the same fibre. In addition for Method 4, the data for each pair that observed the same object are combined.

Method 3M is an alternative mean-sky technique, which is similar to Method 3 except only 10% to 20% of the time is spent observing the sky and the sky spectra are combined.

Comparing the methods

The mean-sky methods, 1, 2 and 3M, have a higher survey efficiency compared to Methods 3 and 4. The relative efficiency can be above 2.0 because there are two gains over a beam-switching method: (i) more fibres are observing objects; and (ii) the S/N per object per exposure time is higher because of the averaging of the sky background.

The advantage of the beam-switching methods is that the sky is observed through the same fibres as the object. This is better for reducing systematic effects caused by, for example, errors in measuring the fibre transmittance and fibre-to-fibre PSF variations. Typically sky-subtraction residuals will be present around OH-emission lines when a mean-sky method is used rather than beam switching[4].

Methods 1, 2 and 4 sample temporal variations in the sky continuously. For Methods 3 and 3M, switching between sky and object exposures must be fast enough to avoid introducing noise due to temporal variations of the sky background[22].

In principal, Method 2 could best sample spatial variations in the sky by judiciously placing each sky fibre within the field. However, it would require a different mechanical arrangement for GIRMOS than with the other methods. Therefore, as long as the spatial sampling of the sky is adequate with the other methods, GIRMOS need not be designed with deployable individual fibres. Ramsay et al. found no significant variation over 90 arcseconds which suggests that the ability to use Method 2 is an unnecessary luxury.

Which method to use?

The choice is between a mean-sky method for high survey efficiency or a beam switching method to minimise systematic errors.

Method 1 is a static mean-sky method. Care must be taken to avoid placing the sky IFUs on non-target, particularly extended astronomical sources. In addition to high survey efficiency, there is no time spent slewing the telescope to different parts of the sky as with a beam switching method or Method 3M. This method could be used when no significant information is required from the OH-line regions and the accuracy of the continuum-background subtraction is not required to be high.

Method 2 is also a static mean-sky method with better spatial sampling than Method 1. However, the improvement may not warrant the extra mechanical complication.

Method 3M is a non-static mean-sky method. In general, there will be no improvement over a static method and there will be noise introduced due to temporal sky variations. However, when a field is very crowded, it may be impossible to use a static method and this method could be used because the sky can be sampled further away. In addition, there is the possibility of using a partial mean-sky method where, for example, the sky is only averaged for each IFU individually. This has the advantage that the PSF variations and the relative fibre-transmittance uncertainties will be less than when averaging the sky over all the IFUs. The partial mean-sky method is a compromise between a full mean-sky method and a beam switching method.

Method 3 is a beam switching method. It has the advantage of the sky and object being taken through the same fibre for each extracted spectrum. There will be noise due to temporal sky variations. This noise can be reduced by switching between sky and object measurements at a higher rate, possibly at the expense of duty cycle and read noise.

Method 4, the cross beam switching method, is generally the best method for reducing systematic errors associated with sky subtraction. Temporal sky variations and errors in fibre transmittance have little effect with this method. Cuby & Mignoli[4] noted that there would be a second-order effect only, “as a product of two first order errors (temporal sky variation and transmission determination)”. This method is the preferred beam-switching technique except in a crowded field where there are problems choosing appropriate sky positions.

The best method depends somewhat on the science case. For example, if a survey only requires Doppler shift measurements from non-OH wavelength regions, then, a mean sky method is entirely adequate. On the other hand, if precise equivalent-width measurements need to be made on the spectra, then, reducing sky residuals becomes important and a beam switching method is better.

GIRMOS should have the ability to use mean-sky methods (1 and 3M) and beam-switching methods (3 and 4). Of most importance will be the development of software to cope with these methods: telescope control, detector-array control and reduction software. Reduction software should include the ability to deal with effects such as localised and uniform scattered light[28]. This will improve sky subtraction with all the methods, but particularly with the mean-sky methods.

Acknowledgments

Gillian Wright, Ray Sharples, Ian Parry, Joss Bland-Hawthorn, Gemini, Anglo-Australian Observatory, UKATC, University of DURHAM.

REFERENCES

1. Allington-Smith J., Content R., "Sampling and background subtraction in fiber-lenslet integral field spectrographs", **PASP, 110**, p. 1216-1234, 1998.
2. Content R., "Advanced image slicers from the laboratory to NGST", **ASP Conf. Ser., Vol. 195,** p. 518–539, 2000.
3. Coude du Foresto V., "Optical fibers in astronomical interferometry", **ASP Conf. Ser., Vol. 152,** p. 309-319, 1998.
4. Cuby J. G., Mignoli M., "Sky subtraction with fibers", in Proc. **SPIE, 2198**, p. 98-109, 1994.
5. Dallier R. Baudrand J, Cuby J. G., "Near IR fiber spectroscopy: First results", **ASP Conf. Ser., Vol. 37,** p. 310- 32o, 1993.
6. Gillingham P., Jones D., "Optical design for IRIS2: the ATT's next infrared spectrograph", **SPIE, 4008** , these proceedings.
7. Gray P. M., Taylor K., Parry I. R., Lewis I. J., Sharples R. M., "The AAT 2df project – current status",, **ASP Conf. Ser., Vol. 37,** p. 145-165, 1993.
8. Guerin J., "AOIFU: AOB OSIS infrared fiber unit", **ASP Conf. Ser., Vol. 152,** p. 282-288, 1998.
9. Haynes R., Lee. D., Allington-Smith. J. R., et al., "Multiple-object and integral field near-infrared spectroscopy using fibers", **PASP, 111,** p. 1451-1468, 1999.
10. Hodapp K., "Infrared detector array: Current state of the art", **SPIE, 4008** , these proceedings.
11. Jones D. H., Bland-Hawthorn J., Burton M. G., "Numerical evaluation of OH airglow suppression filters", **PASP, 108,** p.929, 1996.
12. Larkin J. E., Quirrenbach A., Graham J. R., "Image slicing with infrared fibres", **ASP Conf. Ser., Vol. 195,** p. 508-517, 2000.
13. Lee D., Taylor K., "Fiber development at the Anglo-Australian Observatory for SPIRAL and AUSTRALIS", **SPIE, 4008** , these proceedings.
14. Levin K. H., Trans D. C., Kindler E., Glenar D., "Infrared fiber arrays for low background infrared astronomy", **ASP Conf. Ser., Vol. 37,** p. 295-309, 1993.
15. Lissandrini C., Cristiani S., La Franca F., "Sky subtraction with fiber spectrographs", **PASP, 106,** p. 1157-1164, 1994.
16. Maihara T., Iwamuro F., Yamashita T., Hall D. N. B., Cowie L. L., Tokunaga A. T., Pickles A., "Observations of the OH airglow emission", **PASP, 105**, p.940-944, 1993.
17. Murphy T. W., Jr,. Matthews K., Soifer B. T., "The new palomar integral field spectrograph", **ASP Conf. Ser., Vol. 195,** p. 200-205, 2000.
18. Offer A. R., Bland-Hawthorn J., "Rugate filters for OH-suppressed imaging at near-infrared wavelengths", **MNRAS, 299,** p. 176-188, 1998.
19. Oliva E., Origlia L., "The OH airglow spectrum - a calibration source for infrared spectrometers", **A&A, 254,** p.466, 1992.
20. Parry I., "The astronomical uses of optical fibers", ", **ASP Conf. Ser., Vol. 152,** p. 3-13, 1998.
21. Parry I., Dean A. J., Ellis R. S., et al., "CIRPASS: A near-IR intergral field spectrograph", **ASP Conf. Ser., Vol. 195,** p. 191-195, 2000.
22. Ramsay S. K., Mountain C. M., Geballe T. R., "Non-thermal emission in the atmosphere above Mauna Kea", **MNRAS, 259,** p. 751-760, 1992.
23. Sanghera J. S., Aggarwal I. D., "Infrared fiber optics", **CRC Press LLC,** 1998.
24. Watson F., Offer A. R., Lewis I. J., Bailey J. A., Glazebrook K., "Fiber sky subtraction revisited", **ASP Conf. Ser., Vol. 152**, Fiber Optics in Astronomy III, p. 50, 1998.
25. Wells M. Ramsay-Howat S. K., Hastings P. R., "Design and testing of a cryogenic image slicing IFU for UKIRT and NGST", **SPIE, 4008** , these proceedings.
26. Wright G. S., "Multiple deployable integral field units in the near-IR", ", **ASP Conf. Ser., Vol. 195,** p.165-172, 2000.
27. Wright G. S., Sharples R. M., et al., "GIRMOS: an infrared multiobject spectrograph for Gemini", **SPIE, 4008** , these proceedings.
28. Wyse R. F. G., Gilmore G., "Sky subtraction with fibres", **MNRAS, 257,** p. 1-10, 1992.